Modelling the hydrocarbon generative history of the Officer Basin, Western Australia

K.A.R. Ghori[1]

KEYWORDS: modelling, hydrocarbon, generation, Officer Basin, Western Australia

Abstract

Minor oil shows and numerous bitumen occurrences indicate hydrocarbon generation and migration within the Neoproterozoic Officer Basin of Western Australia. Since thin but organic-rich beds with excellent to fair oil generating potential are present, as are good reservoir and seal rocks, the hydrocarbon generative history of the region is crucial in assessing its petroleum prospectivity.

The hydrocarbon generative history of the region based on multi-dimensional basin modelling of geological sections drawn from wells and seismic shows the vast differences in timing and levels of kerogen transformation to petroleum in the Brown, Hussar, Kanpa, and Steptoe formations. It indicates that the main phases of oil generation within the Neoproterozoic succession was during the latest Neoproterozoic, Cambrian and Permian-Triassic. These phases vary both stratigraphically and geographically across the basin due to variations in at least three major structuring events – the Neoproterozoic Areyonga Movement and Petermann Ranges Orogeny, and the Carboniferous Alice Springs Orogeny – which had a profound affect on depositional and structural history. For these reasons the present-day depth of oil-window within the Neoproterozoic is about 1000 m deeper in the Yowalga area (Kanpa-1A and Yowalga-3) as compared to the Gibson area (Hussa-1). The extent to which later tectonic events affected the basin is poorly known.

The optimum maturity for maximum rate of hydrocarbon generation within the Browne Formation was reached soon after deposition, and most of its hydrocarbon generative potential was exhausted during the Neoproterozoic. However, the overlying Hussar, Kanpa, and Steptoe formations were not buried as deeply, so their hydrocarbon generative potential was not exhausted during the Neoproterozoic.

Introduction

Basin modelling is a powerful tool to test and analyse various geological concepts within the poorly explored Western Australian part of the Officer Basin. The basin is elongate with a northwest-southeast trend, and contains over 8000 m of Neoproterozoic strata (Officer Basin) overlain by lower Palaeozoic rocks of the Gunbarrel Basin. One of the major explorations risks affecting petroleum formation and preservation within the Officer Basin (Fig. 1) is its long and complex evolution, and which can be evaluated from basin modelling. Subsurface geochemical and geological information available within the Gibson, Lennis, Savory, Waigen, and Yowalga areas of the basin, are limited to 16 wells and 19 seismic surveys undertaken during the three phases of petroleum exploration: late 1960s (five wells), early 1980s (five wells), and late 1990s (six wells). Of these areas the Yowalga area contains the most wells: Brown-1 and 2, Empress-1/1A, Kanpa-1A, Lungkarta-1, and Yowalga -1, 2, and 3. The Gibson area contains two deep wells – Hussar-1 and Dragoon-1 – and the remaining wells are of limited use as they are less than 200 m deep. The Neoproterozoic of the Lennis area has no well information whereas in the Waigen area the only available stratigraphic and maturity data, from a single 2016 m deep stratigraphic well (GSWA Vines-1), but are poorly constrained at present.

Fig. 1. The western Officer Basin, showing location of wells and seismic pseudowells utilized in this study for modelling.

[1] Geological Survey of Western Australia
Department of Mineral and Petroleum Resources
Mineral House, 100 Plain Street
East Perth, Western Australia 6004
Email: ameed.ghori@mpr.wa.gov.au

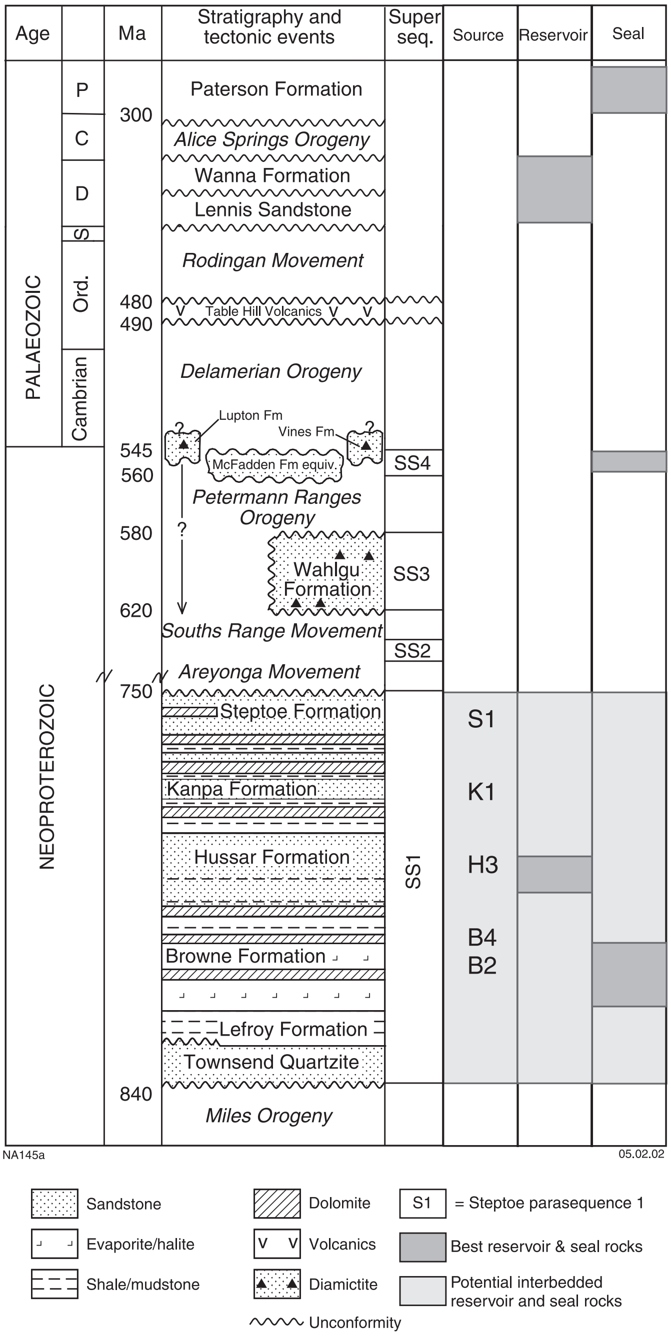

Fig. 2. Generalised time-stratigraphy, source, reservoir and seal rocks of the Officer Basin, Western Australia.

Deep wells and pseudowell locations from seismic sections were modelled, utilising petroleum systems modelling software of Platte River Associates, to calculate the timing of petroleum generation and migration in the basin. The modelling was performed in three steps: (i) 1D modelling of a single well location, utilising version 7.06 of BasinMod 1D; (ii) 1D modelling of multi-well locations, in version 7.06 of BasinView and; (iii) 2D modelling of a cross section using version 4.17 of BasinMod 2D.

The objective in modelling the maturation and hydrocarbon generation history of the Neoproterozoic Officer Basin was to estimate the timing of optimum maturity for maximum hydrocarbon generation reached at different stratigraphic levels and geographic locations. Evaluation of the Gibson and Lennis areas is based on 1D modelling of the single well, whereas the evaluation of the Yowalga area is based on multi-dimensional modelling of available wells.

Geological history

Figure 2 summarises generalised time-stratigraphy, source, reservoir, and seal rocks of the western Officer Basin compiled from many studies, the most important of which are: Jackson et al. (1984), Phillips et al. (1985), Townson (1985), Walter and Gorter (1994), Williams (1992, 1994), Walter et al. (1995), Perincek (1996). Three major Neoproterozoic units are present within the Western Australian part of the basin: Supersequence-1, 3 and 4 (Fig. 2). Of these, Supersequence-1 is the thickest as well as most prospective for petroleum exploration. The mainly clastic Townsend Quartzite and Lefroy Formation are the oldest Neoproterozoic units, and are unconformably overlain by thick evaporite, carbonate and shale units of the Browne, Hussar, Kanpa, and Steptoe formations, in ascending order. Apak and Moor (2000a and b) divided the Brown, Hussar, Kanpa, and Steptoe formations into following genetically correlatable sedimentary parasequence sets: B1-B6, H1-H5, K1-K2, and S1-S2, respectively. The Areyonga Movement, at the end of deposition of Supersequence-1, is the first major Neoproterozoic tectonic episode, which was followed by the Souths Range Movement (Townson, 1985; Perincek 1996; Apak and Moor, 2000a & b).

Supersequence-3 (Wahlgu Formation), comprising sandstone and diamictite in Empress-1/1A, unconformably overlies Supersequence-1. The second major episode of Neoproterozoic tectonic deformation – the Petermann Ranges Orogeny – postdates the deposition of Supersequence-3. In the subsurface, Supersequence-4 (McFadden Formation equivalent) comprises very fine- to coarse-grained clastics, unconformably overlying Supersequences-1 and 3 (Perincek 1996). Besides McFadden Formation equivalent, Lupton Formation from outcrop and Vines Formation in Vines-1 are also equated with Supersequence-4.

The Ordovician Table Hill Volcanics, a widespread, thin, plateau basalt unconformably above the Neoproterozoic succession, marks a new depositional succession that has been formally assigned to the Gunbarrel Basin (Hocking, 1994), and has been related to the Cambrian Delamerian Orogeny (Perincek, 1996). The unconformity at the base of overlying undated massive sandstones of shallow marine origin (Lennis and Wanna Sandstones) is attributed to the Ordovician-Silurian Rodingan Movement (Perincek, 1998). The final Palaeozoic event recognised is the Alice Springs Orogeny, which separates the Upper Carboniferous-Lower Permian Paterson Formation from older units. Tillites and fluvioglacial to lacustrine sandstone and claystone of the Paterson Formation are widespread and equated with the Grant Group of the Canning Basin to the northwest (Jackson and van de Graaff, 1981; Phillips et al., 1985; Townson, 1985). The mid-Carboniferous Alice Springs Orogeny is considered to be the most intensive tectonic episode of the Palaeozoic and reactivated diapiric movements within the Browne Formation and folded the Table Hill Volcanics and

Well	Depth (m)	Sample	TOC (%)	T_{max} (°C)	S_1	S_2	S_3	$S_1 + S_2$	PI	HI	OI
Empress-1A	587.9	core	1.38	418	0.43	6.20	0.11	6.63	0.06	449	8
Empress-1A	588.4	core	1.52	413	0.46	6.44	0.15	6.90	0.07	424	10
Empress-1A	768.2	core	0.93	421	0.66	4.02	0.44	4.68	0.14	432	47
Kanpa-1A	3412.2	swc	1.41	436	1.78	4.83	0.75	6.61	0.27	343	53
NJD-1	327.5	core	6.64	430	0.7	23.47	1.04	24.17	0.03	353	16
NJD-1	328.5	_	3.18	432	0.26	15.83	0.39	16.09	0.02	498	12
NJD-1	400.8	_	1.22	443	0.74	1.27	0.10	2.01	0.37	104	8
NJD-1	502.6	_	21.50	*442	32.11	104.00	1.94	136.11	0.24	484	9
NJD-1	502.7	_	1.10	*430	1.06	4.76	0.45	5.82	0.18	433	41
Normandy LDDH-1	222.8	core	1.61	450	0.42	2.11	0.32	2.53	0.17	131	20
Normandy LDDH-1	529.6	core	2.05	471	1.05	1.40	0.07	2.45	0.43	68	3
Throssell-1	184.9	core	1.37	428	0.35	1.06	0.31	1.41	0.25	77	23
Yowalga-3	1484.0	cuttings	1.23	421	0.49	3.00	0.47	3.49	0.14	244	38

Notes: TOC = total organic carbon; T_{max} = temperature of maximum pyrolytic yield (S_2); S_1 = existing hydrocarbons (HC); S_2 = pyrolytic yield (HC); S_3 = organic carbon dioxide; $S_1 + S_2$ = potential yield; PI = production index; HI = hydrogen index; OI = oxygen index; *Bitumen rich samples

Table 1. TOC and Rock-Eval data for samples with TOC content over 0.90%.

Well	Quality of show	Formation	Formation age
Boondawari-1	40% oil fluorescence in core	Spearhole Formation	Neoproterozoic
Browne-1	Gas cut mud, cut fluorescence, trace oil in core	Paterson Formation	Permian
		Browne Formation	Neoproterozoic
Browne-2	Gas cut mud, cut fluorescence, trace oil in core	Paterson Formation	Permian
Dragoon-1	Mud gas to 10% methane equivalent, including	Browne Formation	Neoproterozoic
	hydrocarbons up to pentane		
Hussar-1	Mud gas readings to 1000 ppm. Possible gas blow	Kanpa Formation	Neoproterozoic
	on air lift. Trip gas to 4.6% total gas. 72% oil	Hussar Formation	
	saturation from log analysis		
Kanpa-1A	Dull yellow-orange sample fluorescence,	Kanpa Formation	Neoproterozoic
	light yellow-white cut fluorescence, brown oil		
	stains in sandstone and dolomite cuttings		
LDDH-1	Bitumen in core	Tarcunyah Group	Neoproterozoic
Mundadjini-1	10% oil fluorescence in core	Spearhole Formation	Neoproterozoic
NJD-1	Bleeding oil and bitumen in core	Neale Formation	Neoproterozoic
OD-23	Bleeding oil and bitumen in core	Scorpion Group	Mesoproterozoic
Vines-1	Total gas peaks 25 times background	?Supersequence 1	Neoproterozoic

Table 2. Oil shows, Officer Basin, Western Australia.

Lennis Sandstone in the Yowalga and Lennis areas (Perincek, 1996). Subsequent erosion led to an angular unconformity between the Permian Paterson Formation and the underlying units (Townson, 1985). Flat-lying Lower Cretaceous interbedded sandstones and claystones of marine origin (Samuel Formation and Bejah Claystone) blanket the northwestern portion of the basin (Phillips et al., 1985). The effects of Mesozoic tectonic events (Jurassic break-up) and the Tertiary (Miocene) are poorly documented within the study area.

Petroleum Geochemistry

The geochemical evaluation is based on data from open-file company reports (Perincek, 1998), analyses of existing samples by Japan National Oil Company (JNOC; 1997) and the Geological Survey of Western Australia (GSWA; Ghori, 1998a, 1998b, 1999, 2000; Hegarty et al, 1988), and new GSWA stratigraphic coreholes (Ghori, 1998c, 1999). The data include total organic carbon analyses (2896), Rock-Eval pyrolysis (694), pyrolysis-gas chromatography (31), rock extract analyses (110), and organic petrology (174).

Source-rock potential

Total organic carbon (TOC) content and Rock-Eval pyrolysis quantifies organic richness and hydrocarbon-generating potential of source beds, whereas Rock-Eval pyrolysis, pyrolysis-gas chromatography (PGC), extraction, liquid (LC) and gas chromatography (GC) identify the type of kerogen or facies. These data show oil and gas prone source beds with fair to excellent hydrocarbon-generating potential are present in

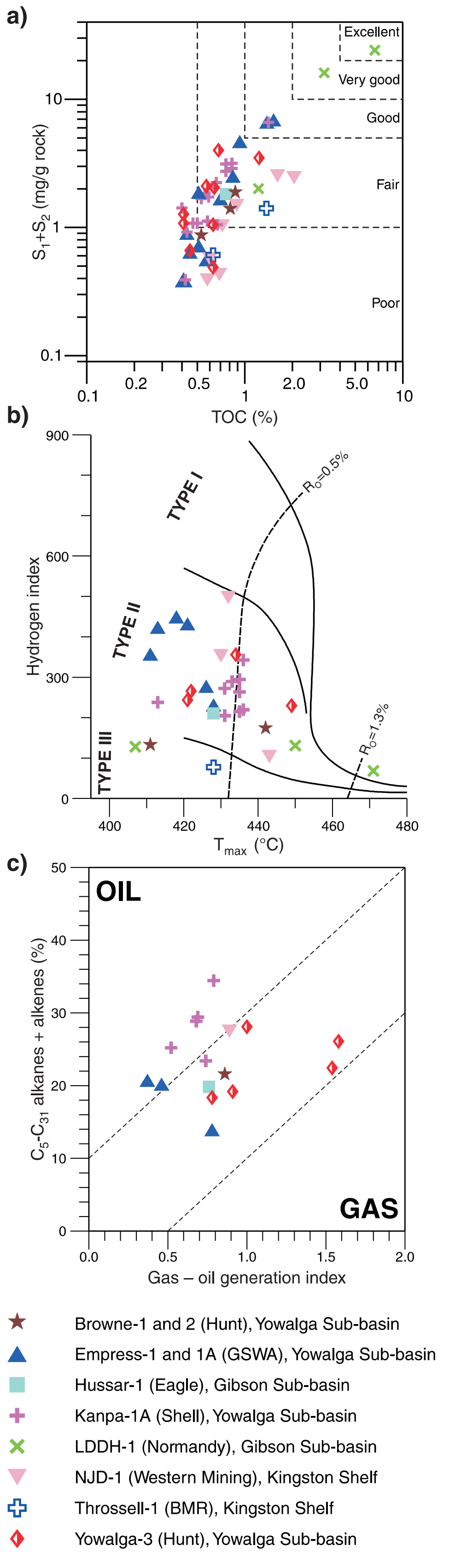

Fig. 3. Source-rock characterisation: a) petroleum-generating potential as a function of organic richness versus potential yield, for samples interpreted as reliable; b) type of kerogen as a function of T_{max} versus hydrogen index, from Rock-Eval pyrolysis; c) type of kerogen as a function of oil proneness (C_5-C_{31} alkanes + alkenes) versus gas-oil generation index (C_1-C_5)/C_{6+}), from pyrolysis-gas chromatography.

Browne-1 and 2, Empress-1/1A, Hussar-1, Kanpa-1A, LDDH-1, NJD-1, Throssell-1, and Yowalga-3.

The best source beds identified in the area are from NJD 1 and Empress-1/1A, which have excellent to good organic richness and generating potential. Such organic rich beds are present within the parasequence sets: B2 and B4, H3, K1, and S1 of the Brown, Hussar, Kanpa, and Steptoe formations, respectively. Figure 3 summarises source rocks characteristics, based on detailed source-rock evaluations in Ghori (2000). Whereas Table 1 provides TOC and Rock-Eval data for samples with TOC content over 0.90%, and Table 2 provides the type of hydrocarbon shows recorded within the Officer Basin of Western Australia, although minor but significant in indicating existence of petroleum system.

Source-rock maturity

Organic petrology and T_{max} from Rock-Eval provide measured thermal maturity, whereas apatite fission-track analysis (AFTA) provides maximum palaeotemperatures and the time of cooling from these temperatures. Finally, organic maturity and timing of hydrocarbon generation from source rocks was estimated from basin modelling. No direct method is available to measure expulsion efficiency.

Organic petrology: Organic petrology for 174 samples from ten wells is available for evaluating source rock maturity. The data provide equivalent vitrinite reflectance obtained from reflectance measurements on fluorescing and non-fluorescing lamalginite, reservoir and thucholitic bitumen, and their fluorescence intensity provide measures of source rock maturity. A plot (Fig. 4a) of equivalent vitrinite reflectance versus depth suggest that most of samples are within the oil generative window, except the basal part of the section within Dragoon-1, Empress-1/1A, LDDH-1, and Yowalga-3.

Rock-Eval pyrolysis: T_{max} is a maturation parameter in °C at which the pyrolytic yield of hydrocarbons (from a rock sample) reaches its maximum. The production index (PI) is also a maturation parameter, and is the ratio of already generated hydrocarbon (S_1) to potential hydrocarbon (S_2). Rock-Eval, T_{max} and PI values for samples with source potential plotted versus depth (Fig. 4b) show that all samples, except those from the basal part of LDDH-1 within the Gibson area, are either immature or within the oil-generative window. The Rock-Eval maturity parameters confirm that the Neoproterozoic within the study area is not overmature for oil generation. The Neoproterozoic section penetrated in the Gibson area is comparatively more mature then in wells of the Yowalga area, as the oil window in Kanpa-1A and Yowalga-3 is about 1000 m deeper than in Hussar-1.

Apatite Fission Track Analysis (AFTA): The fission-track age is largely a function of fission-track annealing in response to increasing temperature between 70°C and 120°C, whereas fission-track length reflects the style of cooling. Apatite fission track analysis therefore complements maturity data in evaluating the geothermal history of the host rocks. Based on fission-track data for ten cuttings samples from Kanpa-1A (5) and Yowalga-3 (5), Green and Gleadow (1984) suggest that most of the

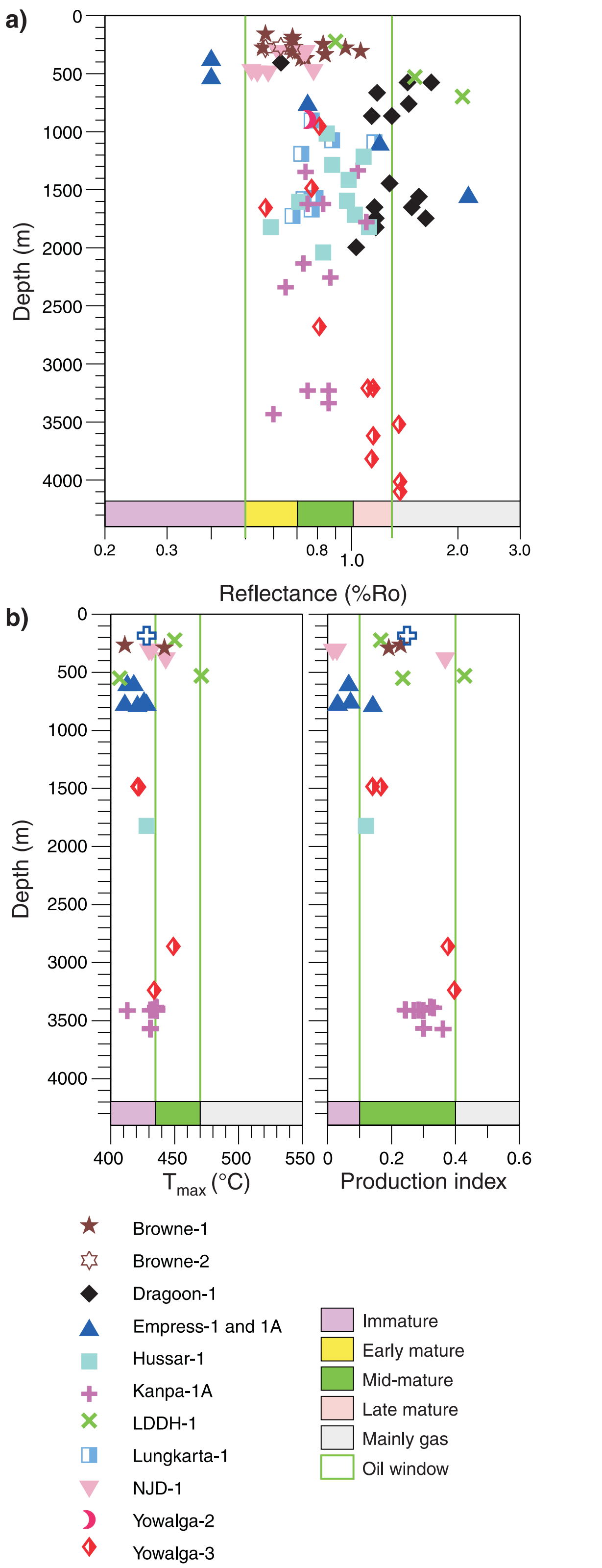

Fig. 4. Measured maturity: a) as a function of equivalent vitrinite versus depth; b) as a function of the Rock-Eval parameters, T_{max} and production index, versus depth.

Neoproterozoic section in those wells may have been mature to overmature relatively early in the history of the basin. AFTA data available on three samples from Empress-1/1A indicate cooling events between 600–300 Ma and between 40 Ma to present (Hegarty et al, 1988), encompassing the Petermann Ranges Orogeny, Alice Springs Orogeny, and Tertiary erosion.

Basin Modelling

Basin modelling is used to analyse different geological scenarios for the evolution of the Officer Basin because the complex burial, thermal, and erosional histories are poorly constrained. The emphasis was to determine the timing of hydrocarbon generation and how sensitive the modelling is to variations in thermal and erosional history, modelling sensitivity was tested on the thickest Neoproterozoic sequence in the Lennis area as interpreted from the available seismic data (Apak and Moors, 2001; Ghori, 2001).

For this study, a total of five wells and seven geological sections from seismic were modelled to reconstruct the hydrocarbon generative history. Wells include Empress-1/1A, Kanpa-1A, Lungkarta-1, and Yowalga-3 plus six pseudowells (derived from seismic data) in the Yowalga area, Hussar 1 from the Gibson area, and a single pseudowell from the Lennis area (Fig. 1). Predicted maturation and timing of hydrocarbon generation are based on Lawrence Livermore National Laboratory (LLNL) vitrinite and kerogen kinetics, respectively. The following options of Platte River BasinMod were used: Bmod 2D fluid flow compaction, power function for permeability calculation, and transient heatflow with 25°C present-day surface temperature for thermal history calculation. Maturation stages and their corresponding vitrinite reflectance values are as follows: immature zone, less than 0.5% Ro; early mature, 0.5% to 0.7% Ro; mid mature, 0.7% to 1.0% Ro; late mature, 1.0% of 1.3% Ro and; mainly gas generation, over 1.3% Ro.

Firstly, 1D burial histories were reconstructed from the stratigraphy and lithologies in wells and estimated for pseudowells. Corrected BHTs, equivalent %Ro, T_{max}, and information from AFTA were used to constrain present-day temperatures and palaeotemperatures. The thermal histories were then reconstructed using estimated erosional histories and adjusting thermal conductivities and transient heat flow to constrain maturity models versus measured data. The stratigraphy and lithologies in wells was taken from Karajas and Taylor (1983a, 1983b), Shell Development (Australia) Pty Ltd (1981), The Shell Company of Australia (1983, 1985), and Stevens and Apak (1999).

For the Yowalga area, the time-stratigraphy utilised is summarised in Table 3, and the maturity calibration and burial histories of three key wells are illustrated in Figure 5. The deepest equivalent vitrinite reflectance value is considered to represent the maximum maturity attained in the wells because the T_{max} values are consistently lower than the equivalent vitrinite reflectance values in this area. The modelling suggest that the K2 parasequence within the Kanpa Formation and underlying formations in Empress-1/1A and Kanpa-1A, and the H4 parasequence within the Hussar Formation and underlying formations in Yowalga-3 are within the mature zone for oil and gas generation.

For the Gibson area, the time-stratigraphy used to model the hydrocarbon generative history was from Hussar-1 (2040 m total

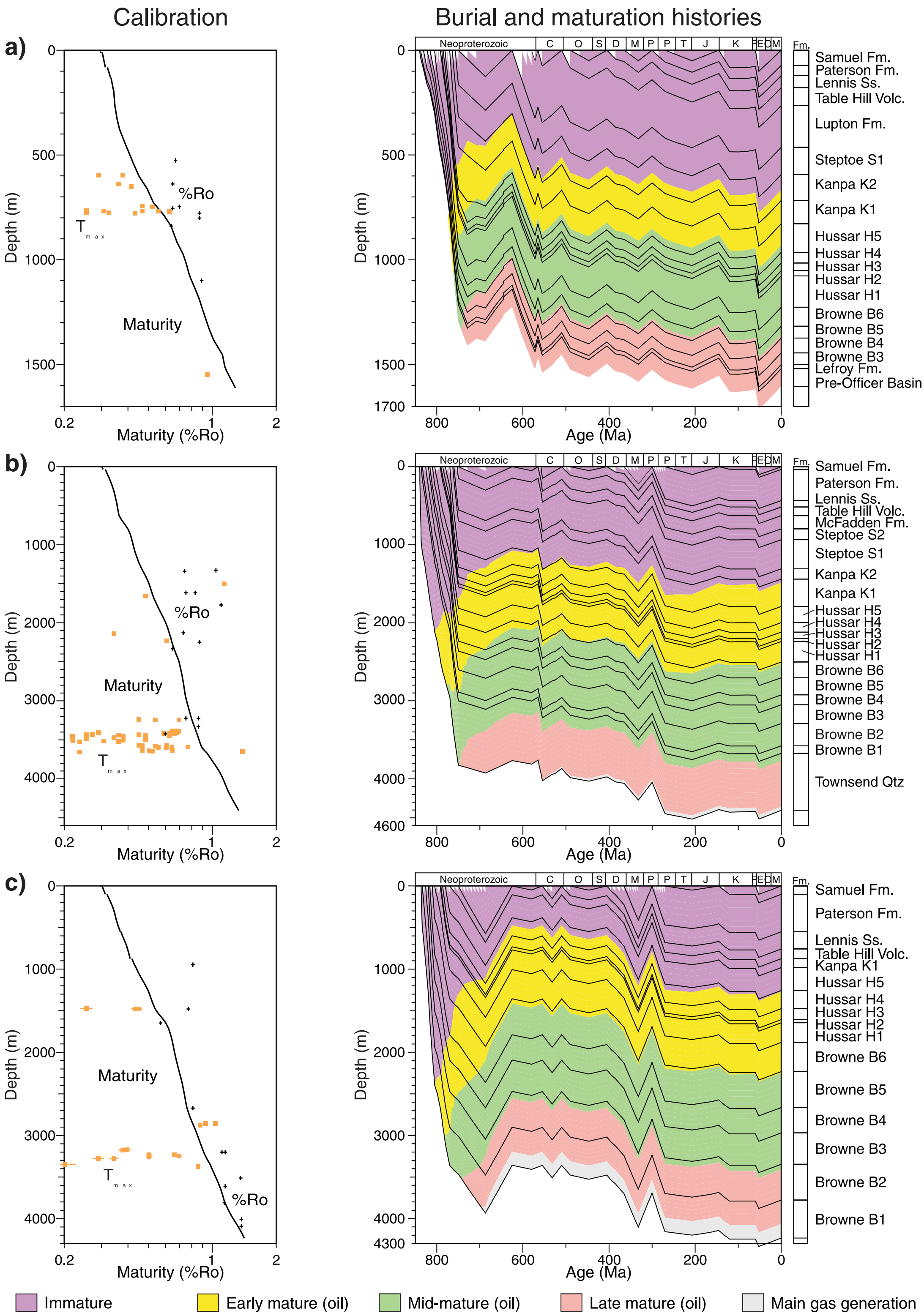

Fig. 5. Calibration of calculated versus measured maturity, and burial and thermal history of three key wells: a) Empress-1/1A; b) Kanpa-1A; c) Yowalga-3.

depth), which was extrapolated from seismic to a total depth of 5405 m and is summarised in Table 4. Modelling of this section is summarized in Figures 6a (maturity calibration) and 6b (burial and maturation history). The corresponding generation timing for the Brown and Hussar formations peaked during the Neoproterozoic and Cambrian, respectively (Figs 6c and 6d).

For the Lennis area, the time-stratigraphy used in developing the pseudowell model is summarised in Table 5. At this location four alternative models, based on available seismic and well data extrapolated from the Yowalga area, were generated to test how variations in thermal and erosional history affect the timing of hydrocarbons generation. The present-day maturity of the

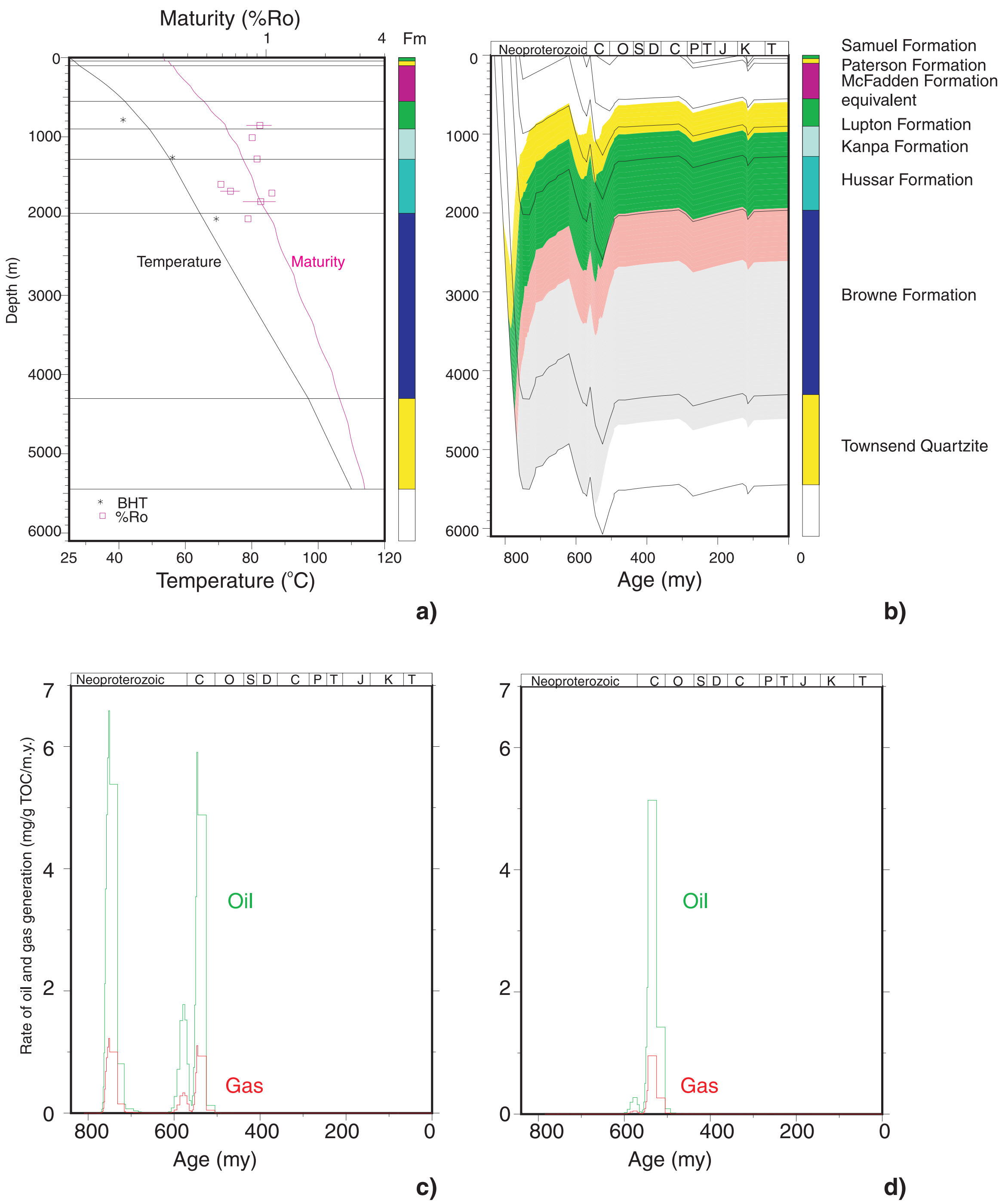

Fig. 6. Hydrocarbon generation modelling of Hussar-1, Gibson area: a) calibration of calculated versus measured maturity; b) burial and thermal history; c) rate of hydrocarbon generation for the Brown Formation; d) rate of hydrocarbon generation for the Hussar Formation.

formations is higher than expected for their current depth of burial, which may be due to either a higher palaeoheat flow or to deeper burial in the past. A higher palaeoheat flow was used to constrain the first two models, whereas deeper burial and erosion were used to constrain the third and fourth models, while keeping the heat flow constant.

To constrain the first model, a high heat-flow value of 67 milliwatts per square metre (mW/m^2) was required for the base of the section at 840 Ma. The heat flow was then reduced at a constant rate to the present-day heat flow (33.7 mW/m^2). For the second model, a constant heat flow of 49 mW/m^2 was used for the section from 840 to 60 Ma (early Tertiary), and then reduced at a constant rate to the present-day heat flow, because AFTA data from Empress-1/1A indicate cooling during the Tertiary.

For the third and fourth models, a constant present-day heat-flow value of 36.3 mW/m^2 was used, with two different scenarios for the erosional history. To constrain the third model, a 1400 m thick section was eroded during the mid-Carboniferous Alice Springs Orogeny. In the fourth model, a 1050 m thick section was eroded during the Late Jurassic break-up of Gondwanaland. Figure 7 illustrates the burial and maturation histories of the

Formation or Event Name	Begin Age (Ma)	Empress 1/1A	Kanpa 1A	Yowalga 3	Lungkarta 1	SP 100 (81-21-AB)	SP 4725 (T82-42)	SP 500 (80-07)	SP 5850 (81-11-E)	SP 2030 (T80-11)	SP 5000 (T81-29)
	120				Cenozoic unconformity						
Samuel Fm	145	0	0	0	0	0	0	0	0	0	0
	270				Mesozoic unconformity						
Paterson Fm	300	79	40	106	88	100	100	100	100	400	30
	365				Alice Springs Orogeny unconformity						
Lennis Ss	405	131	440	555	364	225	225	225	225	1000	430
	490				Rodingan Movement unconformity						
Table Hill Volc	510	201	547	763	540	291	325	650	454	1705	759
	555				Delamerian Orogeny unconformity						
McFadden Fm	565	_	658		704	345	346	659	517	1819	944
	580				Petermann Ranges Orogeny unconformity						
Lupton Fm	625	286	_	_	_	_	_	_	_	_	_
	750				Areyonga Movements unconformity						
Steptoe S2	753	_	829	_	_	595	490	699	658	2011	1842
Steptoe S1	760	483	970	_	_	618	722	772	821	2251	2051
Kanpa K2	763	617	1341	_	809	679	1333	964	1250	2881	2600
Kanpa K1	770	748	1472	880	859	746	1417	1138	1351	3123	2944
Hussar H5	780	860	1817	991	1196	924	1638	1597	1617	3759	3850
Hussar H4	786	981	2020	1267	1400	1137	1926	1763	1830	3975	3937
Hussar H3	790	1030	2140	1485	1578	1264	2096	1861	1956	4102	3989
Hussar H2	792	1065	2220	1617	1682	1348	2209	1927	2040	4187	4023
Hussar H1	805	1105	2259	1655	1722	1389	2264	1959	2081	4228	4040
Browne B6	810	1250	2515	1888	_	1658	2627	2168	2350	4500	4150
Browne B5	816	1340	2712	2228	_	1915	2725	2488	2559	4815	4296
Browne B4	820	1397	2927	2650	_	2196	2832	2837	2787	5159	4454
Browne B3	826	1466	3052	2950	_	2359	2895	3040	2920	5359	4547
Browne B2	834	_	3288	3320	_	2668	3012	3423	3170	5737	4721
Browne B1	836	_	3570	3744	_	3036	3153	3881	3469	6188	4929
Lefroy Fm	838	1521	_	_	_	_	_	_	_	_	_
Townsend Qtze	840	_	3671	np	_	3168	3203	4045	3576	6350	5004
Pre-Officer	_	1540	_	_	_	_	_	_	_	_	_
TD	_	1624	3803	4197	1770	5391	3840	5718	5738	6880	6105

Note: my: million years; Fm: Formation; Ss: Sandstone; Volc: Volcanics; Qtze: Quartzite; TD total depth (m)

Table 3. Time-stratigraphy used in the maturity models of the Yowalga area.

above models based on: a) high heat flow at 840 Ma; b) high heat flow up to the early Tertiary; c) major erosion during the Alice Springs Orogeny; and d) major erosion during the Late Jurassic break-up orogeny. The difference in present-day heat-flow values is due to difference in estimated eroded section and their lithology utilised in these models to constrained the measured versus calculated present-day temperatures and palaeotemperatures.

Finally, the maturity models were used to perform kinetic modelling of petroleum generation as a function of geothermal history, and type and amount of kerogen to determine the timing of hydrocarbon generation, using one-percent organic richness of type II kerogen. Plots of the rate of hydrocarbon-generation versus time for the top of the Browne and Hussar, Kanpa, and Steptoe formations (Figs 8i to iii) indicate that the thicknesses and time of the erosion are the key factors controlling the timing of hydrocarbon generation.

In the second step, the 1D models developed for the Yowalga area were used to develop a multi-well model to estimate the geographic variation in the present-day maturation levels for the parasequences within which source-beds have been identified. Source-beds have been identified within the S1 parasequence of the Steptoe Formation and K1 parasequence of the Kanpa Formation in Empress-1/1A, H3 parasequence of the Hussar Formation and B4 parasequence of the Browne Formation in Yowalga-3, and B2 parasequence of the Browne Formation in Kanpa-1A. Figure 9 illustrates the maturation levels at the surface of the source rock containing parasequences based on the ten 1D models. The modelling suggests that the basal part of the Steptoe Formation is immature in most of the area, except in the northern most part (Fig. 9a), whereas at the base of the Kanpa Formation the maturity reaches to early stages in parts of the area as shown in Figure 9b. The maturity level progressively increases from early to overmature stages in the deeper parasequences and it is higher in the northern part of the study area. Figures 9c, d and e illustrate maturity levels for the H3 parasequence of the Hussar Formation, and B4 and B2 parasequences of the Browne Formation, respectively.

The final step was 2D modelling of a composite cross section from Empress-1/1A in the south to the pseudowell at SP 2030 (Fig. 1) on seismic line T80-11 in the north to estimate

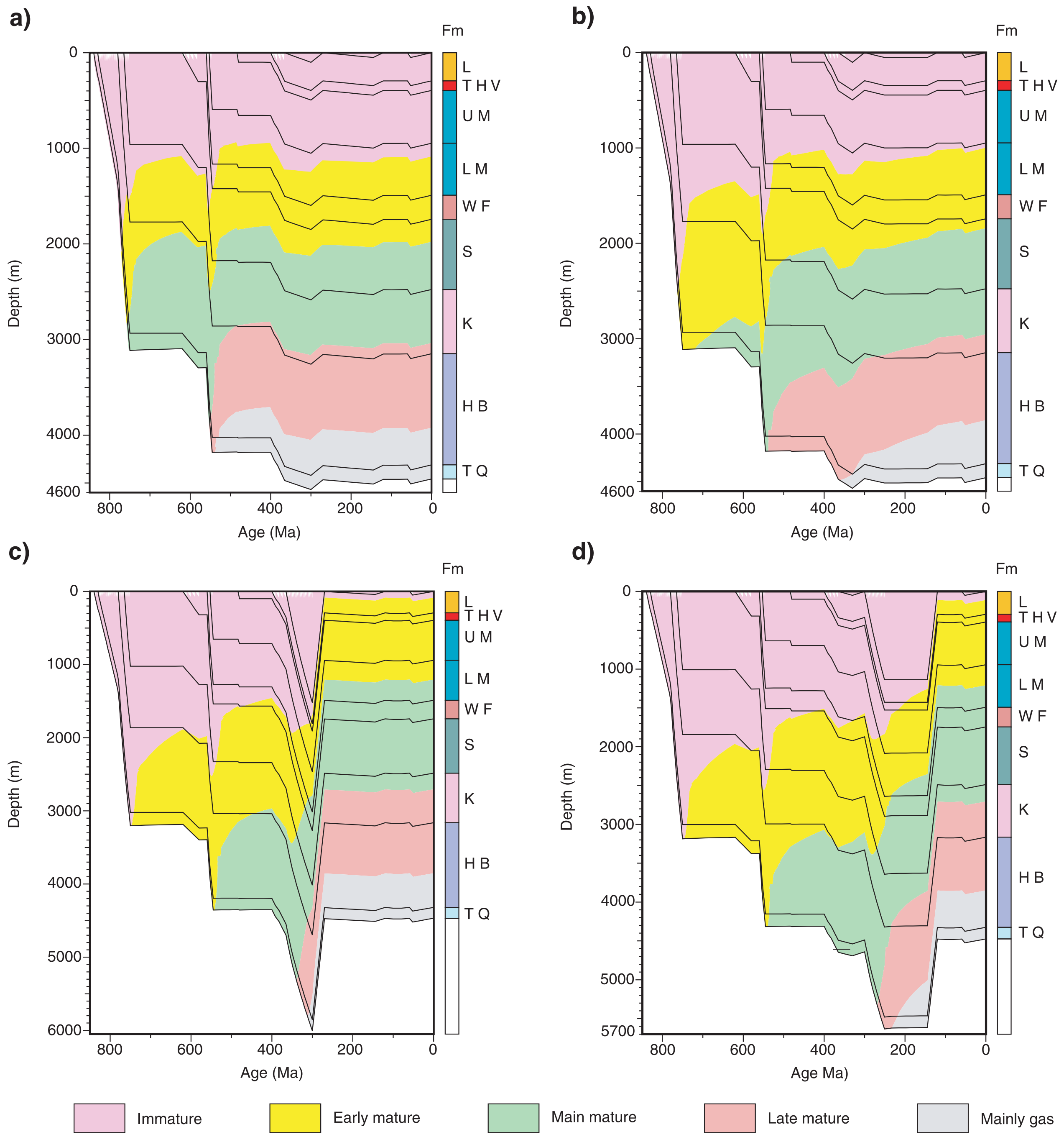

Fig. 7. Burial and maturation histories of models based on: a) high palaeoheat flow at 840 Ma; b) high palaeoheat flow during 840-60 Ma; c) major erosion during the Alice Spring Orogeny; d) major erosion during the Late Jurassic break-up orogeny. The sedimentary sequences indicated on these figures are the Lennis Sandstone (L), Table Hill Volcanics (THV), Upper McFadden Formation equivalent (UM), Lower McFadden Formation equivalent (LM), Wahlgu Formation (WF), Steptoe Formation (S), Kanpa Formation (K), Hussar and Brown formations (HB), and the Townsend Quartzite (TQ).

maturation levels and the timing of hydrocarbon generation across the region. The model was constrained against measured present-day temperatures and maturity, allowing maturation stages reached at different stratigraphic levels across the area to be calculated using lateral variations in the present-day temperatures and palaeotemperatures (Fig. 10).

Kinetic modelling of petroleum generation as a function of geothermal history and type and amount of kerogen was used to determine the timing of hydrocarbon generation, using one-percent organic richness of type II kerogen. Figure 11 illustrates the timing and comparative rate of hydrocarbon generation for three parasequences mature enough to generate hydrocarbons in the three key wells.

Hydrocarbon generation from parasequence B4 in Empress-1/1A, which is the most mature source rock of the modelled wells, peaked during the Neoproterozoic. While the older and deeper B2 parasequence at Kanpa-1A and Yowalga-3 is less mature and at the early stage of hydrocarbon generation, this early maturity was also reached during the Neoproterozoic. Other

Formation or Event Name	Begin Age (Ma)	Formation top (m)	Formation thickness (m)	Missing thickness (m)
Tertiary-Cretaceous unconformity				-100
Samuel Formation	130–120	0	43	
Mesozoic unconformity				-100
Paterson Formation	310–290	43	58	
Alice Springs Orogeny				-120
Rodingan Movement				
Delamerian Orogeny				
McFadden Formation Equivalent	560–545	101	459	
Petermann Ranges Orogeny				-150
Wahlgu Formation	580–620	560	248	
Areyonga Movement				-300
Kanpa Formation	770–760	892	407	
Hussar Formation	785–770	1299	666	
Browne Formation	810–785	1965	2310	
Townsend Quartzite	830–810	4275	1130	

Table 4. Time-stratigraphy used in the maturity model of the Gibson area.

Formation or Event Name	Begin Age (Ma)	Formation top (Ma)	Formation thickness (Ma)	Missing thickness (Ma) Model1	Missing thickness (Ma) Model2	Missing thickness (Ma) Model3	Missing thickness (Ma) Model4
Tertiary unconformity	52			-50	-50	-50	-50
Cretaceous	120	Absent					
Mesozoic unconformity	145			-50	-50	-50	-1050
Paterson Formation	300	Absent					
Alice Springs Orogeny	365			-50	-50	-1400	-50
Lennis Sandstone	400	0	293				
Rodingan Movement	480	Hiatus					
Table Hill Volcanics	484	293	100				
Delamerian Orogeny	545	Hiatus					
Upper McFadden Formation Equivalent	553	393	552				
Lower McFadden Formation Equivalent	560	945	535				
Petermann Ranges Orogeny	580	Hiatus					
Wahlgu Formation	620	1480	248				
Areyonga Movements	750	Hiatus					
Steptoe Formation	765	1728	719				
Kanpa Formation	780	2447	661				
Browne-Hussar formations	830	3108	1142				
Townsend Quartzite	840	4250	150				

Table 5. Time-stratigraphy used in the maturity models of the Lennis area.

parasequences containing source beds in these wells (H3, K1, and S1) are at the earliest stages of oil and gas generation.

The modelling suggest that the highest maturity was reached in the northern part of the Yowalga area. Hence the pseudowell at SP 2030 on seismic line T80-11 is used to illustrate the timing of hydrocarbon generation for the five likely source-rock parasequences (Fig. 12). The modelling clearly demonstrates the vast differences in timings and levels of hydrocarbon generation attained in the Browne, Hussar, Kanpa, and Steptoe formations. At least seven unconformities (Table 3) have affected the hydrocarbon generative history of the area. The Browne Formation was deeply buried and attained the optimum maturity for hydrocarbon generation early during the history of the basin, thus most of its generative potential was exhausted during the Neoproterozoic. By comparison, the Hussar, Kanpa, and Steptoe formations were not buried deeply enough to reached the optimum maturity, and so their hydrocarbon generative potential was not exhausted during the Neoproterozoic. Clearly, the timing of hydrocarbon generation, which is a function of the maximum burial temperatures reach as well as resident time at that temperature of source rock intervals, is spread throughout the geological main phases of the basin evolution.

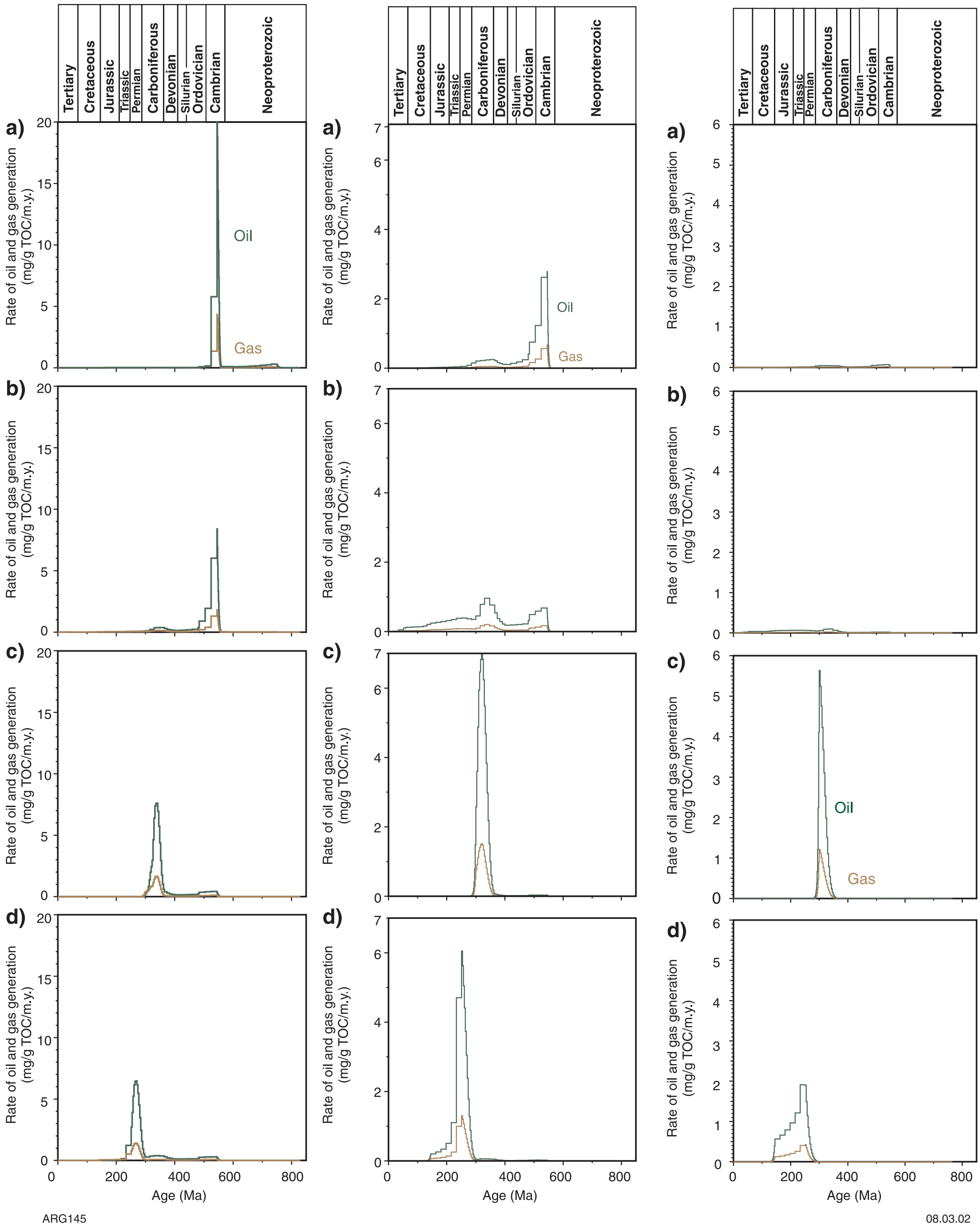

Fig. 8. Rate of hydrocarbon generation for: i) the top of the Browne and Hussar formations for models based on -a) high palaeoheat flow at 840 Ma; b) high palaeoheat flow during 840-60 Ma; c) major erosion during the Alice Spring Orogeny; d) major erosion during the Late Jurassic break-up orogeny. ii) the top of Kanpa Formation for models based on -a) high palaeoheat flow at 840 Ma; b) high palaeoheat flow during 840-60 Ma; c) major erosion during the Alice Spring Orogeny; d) major erosion during the Late Jurassic break-up orogeny. iii) the top of Steptoe Formation for models based on -a) high palaeoheat flow at 840 Ma; b) high palaeoheat flow during 840-60 Ma; c) major erosion during the Alice Spring Orogeny; d) major erosion during the Late Jurassic break-up orogeny.

Conclusions

The available geochemical data identify thin source-beds with fair to excellent hydrocarbon generating potential in Browne-1 and 2, Empress-1/1A, Hussar-1, Kanpa-1A, LDDH-1, NJD-1, Throssell 1, and Yowalga-3. The organic rich source-beds are present within B2 and B4 parasequences of the Browne Formation, H3 parasequence of the Hussar Formation, K1 parasequence of the Kanpa Formation, and S1 parasequence of the Steptoe Formation. Pyrolysis gas chromatography and extract analyses indicate that most the organic matter within the source-beds is of oil and gas generating type II kerogen. The presence of minor oil shows and numerous bitumen occurrences indicate the presence of a petroleum system within the Neoproterozoic of the western Officer Basin.

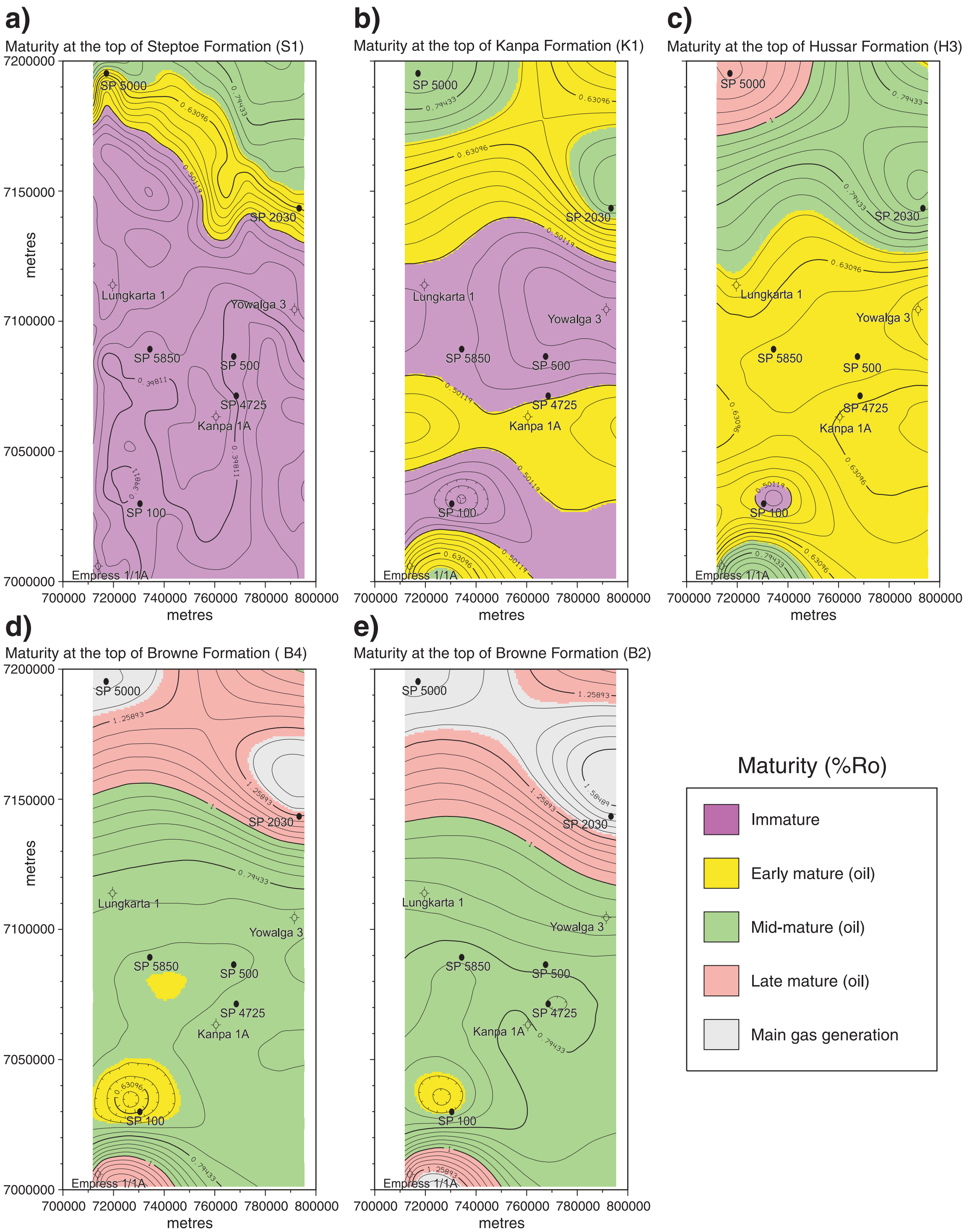

Fig. 9. Maturity at the surface of the five key stratigraphic parasequences: a) S1 of the Steptoe Formation; b) K1 of the Kanpa Formation; c) H3 of the Hussar Formation; d) B4 of the Browne Formation; e) B2 of the Browne Formation.

Organic petrology and Rock-Eval pyrolysis indicates that the measured maturity of the Neoproterozoic succession ranges from immature to overmature. However, a significantly thick Neoproterozoic succession is presently within the oil window that is up to 2000 m thick in Yowalga-3 (where the thickest Neoproterozoic section was penetrated). Thus the present-day depth of oil window in Kanpa-1A and Yowalga-3 (Yowalga area) is about 1000 m deeper than in Hussar-1 (Gibson area).

The hydrocarbon generation modelling suggests that within the Browne Formation the optimum maturity for the maximum rate of hydrocarbon generation was reached early in the basin's history and most of its hydrocarbon generative potential was exhausted during the Neoproterozoic. However, the Hussar, Kanpa, and Steptoe formations were not buried so deeply and hydrocarbon generation from these units extends into the Phanerozoic. The stratigraphic and structural

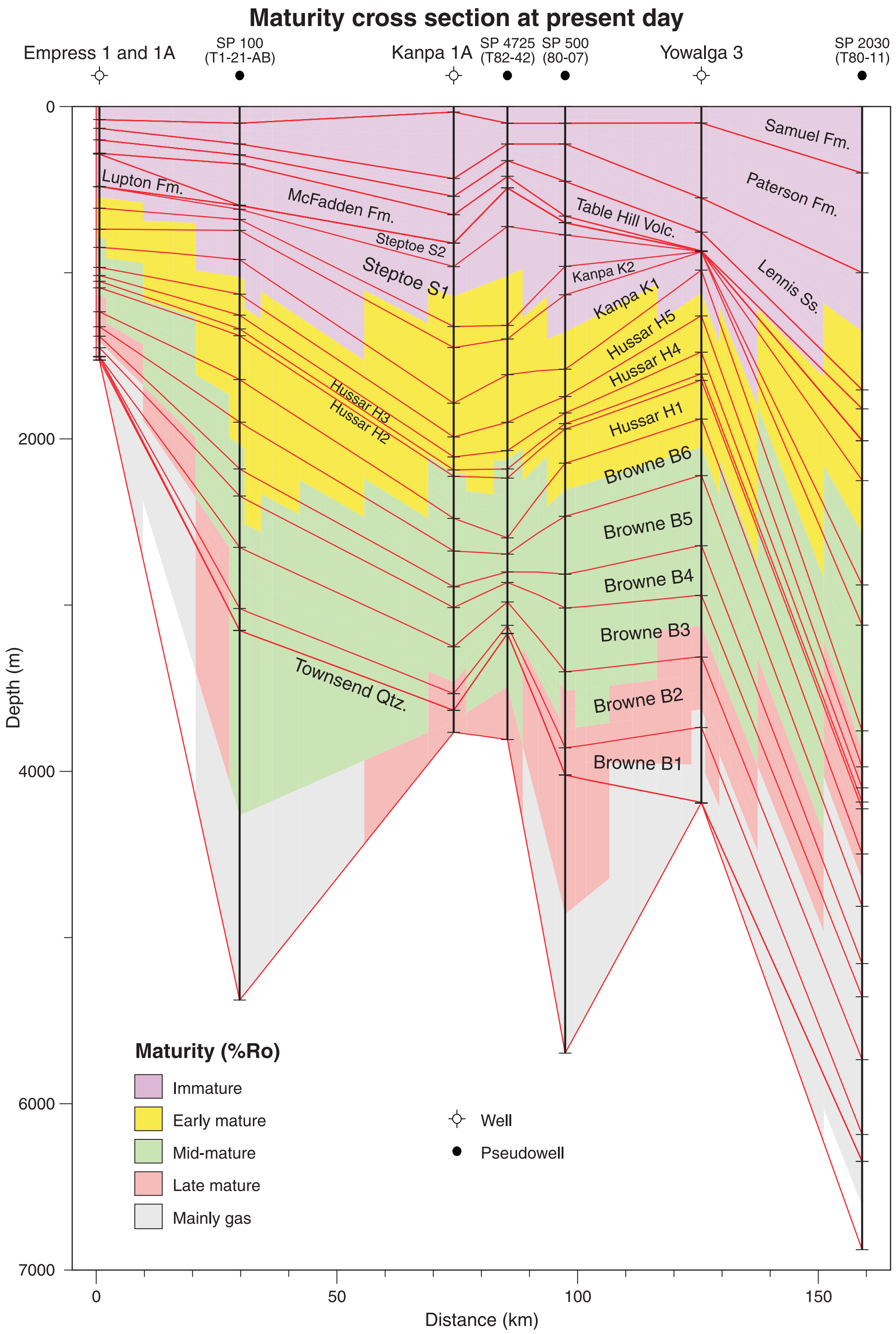

Fig. 10. Present-day maturity across the Yowalga area, from Empress-1/1A in the south to SP 2030 on seismic line T80-11 in the north. The maturity is based on 2D modelling and well locations are shown in Figure 9.

evolution of the basin as well as petroleum formation and preservation were affected by at least seven tectonic events of which the Areyonga Movement, Petermann Ranges Orogeny, and Alice Spring Orogeny had the greatest effect. These tectonic events varied in their effect geographically and stratigraphically and consequently there are considerable variations in the history of hydrocarbon generation across the basin. As similar maturity levels are observed at very shallow depth in parts of the Gibson area (LDDH-1) and salt diapirs (Dragoon-1, Brown-1 and 2), whereas oil window is very deep in Yowalga area (Yowalga-3). The extent and effects of Mesozoic and Tertiary tectonic events are poorly understood, because the preserved post-Alice Spring Orogeny section is thin and irregularly distributed.

The vast area covered by the western Officer Basin is very poorly explored and the sparse well control precludes a complete assessment of the source-rock potential of the Neoproterozoic succession. Effective source rock units and commercially viable petroleum system cannot be identified from the available dataset. However, thin good quality source units has been verified in the Browne, Hussar, Kanpa, and Steptoe formations and that the significant part of the Neoproterozoic section is presently within the oil window and contain good reservoir and seal rocks suggesting further exploration of this frontier region is warranted.

Acknowledgements

I would like to thank my colleagues at Geological Survey of Western Australia for their contributions. This paper is published with the permission of the Director, Geological Survey of Western Australia.

References

APAK, S.N. AND MOORS, H.T., 2000a—A sequence stratigraphic depositional model of Neoproterozoic strata, Yowalga area, Officer Basin, Western Australia. APPEA Journal, 40(1), 15–25.

APAK, S.N. AND MOORS, H.T., 2000b—Basin development and petroleum exploration potential of the Yowalga area, Officer Basin, Western Australia. Western Australia Geological Survey, Report 76, 61p.

APAK, S.N. AND MOORS, H.T., 2001—Basin development and petroleum exploration potential of the Lennis area, Officer Basin, Western Australia. Western Australia Geological Survey, Report 77, 42p.

GHORI, K.A.R., 1998a—Petroleum generating potential and thermal history of the Neoproterozoic Officer Basin. In: Purcell, P.G. and Purcell, R.R. (eds) The Sedimentary Basins of Western Australia. Proceedings of Petroleum Exploration Society of Australia Symposium, Perth, 1998, 717–730.

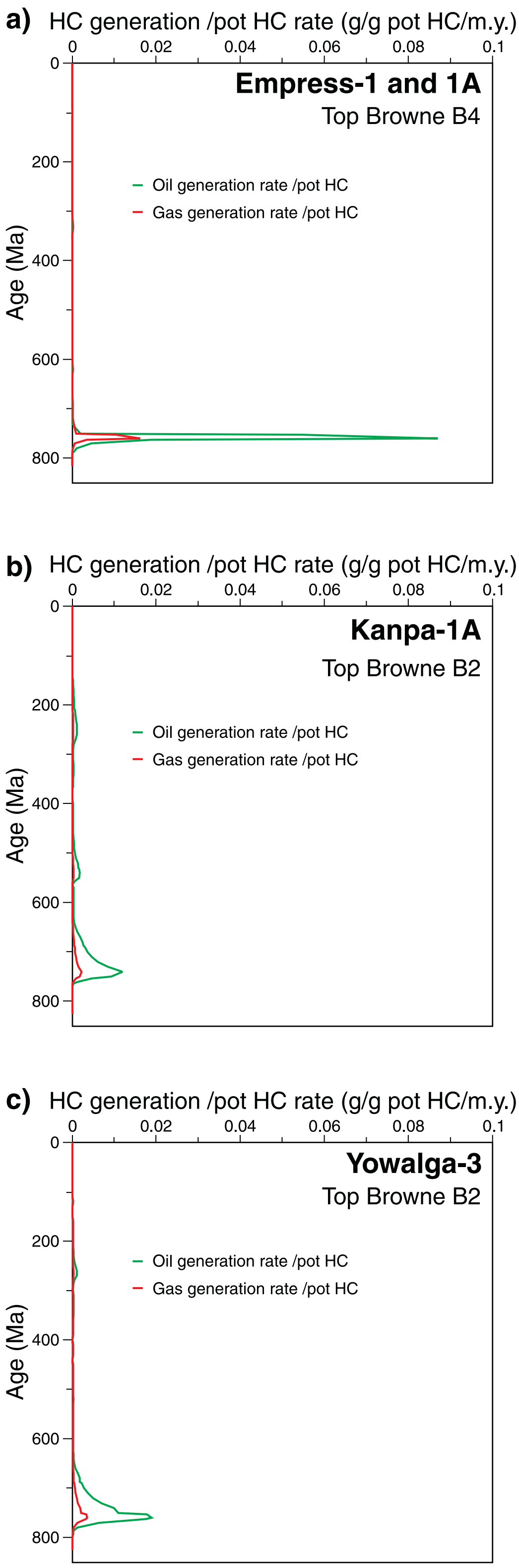

Fig. 11. Rate of hydrocarbon generation versus time for the Browne Formation: a) top B4 parasequence in Empress-1/1A; b) top B 2 parasequence in Kanpa-1A; c) top B2 parasequence in Yowalga-3.

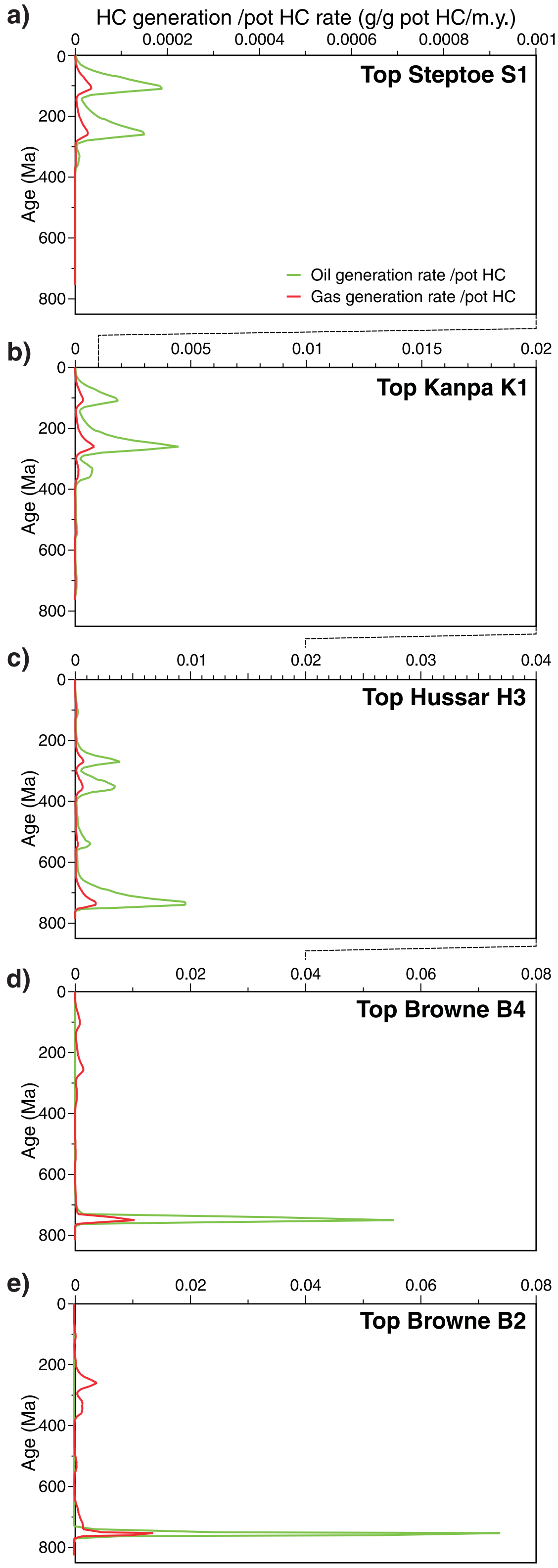

Fig. 12. Rate of hydrocarbon generation at SP 2030 on seismic line T80-11 location for the top of the B2, B4, H3, K1, and S1 parasequences of the Browne, Hussar, Kanpa and Steptoe formations.

GHORI, K.A.R., 1998b—Petroleum source-rock potential and thermal history of the Officer Basin, Western Australia. Western Australia Geological Survey, Record 1998/3, 52p.

GHORI, K.A.R., 1998c—Appendix 5: Geochemistry. In: Stevens, M.K. and Adamides, N.G. (compiler) GSWA Trainor-1 well completion report, Savory Sub-basin, Officer Basin, Western Australia. Western Australia Geological Survey, Record 1996/12, 57–61.

GHORI, K.A.R., 1999—Appendix 9: Geochemistry. In: Stevens, M.K. and Apak, S.N. (compiler) GSWA Empress-1 and 1A well completion report, Yowalga Sub-basin, Officer Basin, Western Australia. Western Australia Geological Survey, Record 1999/4, 73–101.

GHORI, K.A.R., 2000—Appendix: Petroleum source rock potential and maturation history of the Yowalga area. In: Apak, S.N. and Moors, H.T. Basin development and petroleum exploration potential of the Yowalga area, Officer Basin, Western Australia. Western Australia Geological Survey, Report 76, 49–61.

GHORI, K.A.R., 2001—Appendix: Thermal history of the Lennis area. In: Apak, S.N. and Moors, H.T. Basin development and petroleum exploration potential of the Lennis area, Officer Basin, Western Australia. Western Australia Geological Survey, Report 77, 34–42.

GREEN, P.F. AND GLEADOW A.J.W., 1984—Fission track analysis of samples from Kanpa-1A and Yowalga-3, Officer Basin for Shell Development (Australia) Pty Ltd, GEOTRACK International. Western Australia Geological Survey, S-series, Item S3221 A1 (unpublished).

HEGARTY, K.A., O'BRIEN, C. AND WATSON, P.G.F., 1988—Thermal history reconstruction for the Empress 1A well (Officer Basin) using apatite fission track analysis and reflectance by Geotrack International Pty Ltd (GEOTACK), Report 681. Western Australia Geological Survey, S-series 20424 A2 (unpublished).

HOCKING, R.M., 1994—Subdivisions of Western Australian Neoproterozoic and Phanerozoic sedimentary basins. Western Australia Geological Survey, Record 1994/4, 83p.

JACKSON, K.S., McKIRDY, D.M. AND DECKLEMAN, J.A., 1984—Hydrocarbon generation in the Amadeus Basin, Central Australia, APEA Journal 24(1), 42–65.

JACKSON, M.J. AND van de GRAAFF, W.J.E., 1981—Geology of the Officer Basin, Western Australia, Australia Bureau of Mineral Resources, Bulletin 206, 102p.

JAPAN NATIONAL OIL CORPORATION, 1997—Geological and geophysical survey in the western Officer Basin, Western Australia - integrated geological interpretation study. Western Australia Geological Survey, S-series, S10276 (unpublished).

KARAJAS, J. AND TAYLOR, D., 1983a—Dragoon No. 1 well completion report, Eagle Corporation Ltd. Western Australia Geological Survey, S-series, Item S2185 A8 (unpublished).

KARAJAS, J. AND TAYLOR, D., 1983b—Hussar-1 well completion report, Eagle Corporation Ltd. Western Australia Geological Survey, S-series, Item S2242 A4 (unpublished).

PERINCEK, D., 1996—The age of Neoproterozoic-Palaeozoic sediments within the Officer Basin of the Centralian Super-Basin can be constrained by major sequence-bounding unconformities. APPEA Journal, 36(1), 350–368.

PERINCEK, D., 1998—A compilation and review of data pertaining to the hydrocarbon prospectivity of the Officer Basin. Western Australia Geological Survey, Record 1997/6, 209p.

PHILLIPS, B.J., JAMES, A.W. AND PHILIP, G.M., 1985—The geology and hydrocarbon potential of the north-western Officer Basin. APEA Journal, 25 (1), 52-61.

SHELL DEVELOPMENT (AUSTRALIA) PTY LTD, 1981—Yowalga-3 well completion report. Western Australia Geological Survey, S-series, Item S1709 A5 (unpublished).

STEVENS, M.K. AND APAK, S.N. (COMPILERS), 1999—GSWA Empress-1 and 1A well completion report, Yowalga Sub-basin, Officer Basin, Western Australia: Western Australia Geological Survey, Record 1999/4, 110p.

THE SHELL COMPANY OF AUSTRALIA LTD, 1983—Kanpa-1/1A well completion report. Western Australia Geological Survey, S-series, Item S2281 (unpublished).

THE SHELL COMPANY OF AUSTRALIA LTD, 1985—Lungkarta-1 and Lungkarta-1 Sidetrack well completion report (Officer Basin, EP178). Western Australia Geological Survey, S-series, Item S2667 (unpublished).

TOWNSON, W.G., 1985—The subsurface geology of the western Officer Basin results of Shell's 1980–1984 petroleum exploration campaign. APEA Journal, 25 (1), 34–51.

WALTER, M.R. AND GORTER, J.D., 1994—The Neoproterozoic Centralian Superbasin in Western Australia: the Savory and Officer Basins. In: Purcell, P.G. and Purcell, R.R. (eds) The Sedimentary Basins of Western Australia. Proceedings of Petroleum Exploration Society of Australia Symposium, Perth, 1994, 851–864.

WALTER, M.R., VEEVERS, J.J., CALVER, C.R. AND GREY, K., 1995—Neoproterozoic stratigraphy of the Centralian Superbasin, Australia. Precambrian Research, 73, 173–195.

WILLIAMS, I.R., 1992—Geology of the Savory Basin, Western Australia. Western Australia Geological Survey, Bulletin 141, 115p.

WILLIAMS, I.R., 1994—The Neoproterozoic Savory Basin, Western Australia. In: Purcell, P.G. and Purcell, R.R. (eds) The Sedimentary Basins of Western Australia. Proceedings of Petroleum Exploration Society of Australia Symposium, Perth, 1994, 841–850.